# THE EFFECT OF HOT CORROSION ON CREEP AND LOW-CYCLE

# FATIGUE IN THE CAST NICKEL-BASE SUPERALLOY IN738LC

Guo Jianting[*], D. Ranucci[**], and E. Picco[**]

[*]Institute of Metal Research, Academia Sinica,
Wenhua Road, Shenyang, China
[**]Institute of Technology for Non-Traditional
Metals-C.N.R., Via Induno 10, I-20092,
Cinsello, Balsamo (Milano), Italy

## Summary

The creep and low cycle fatigue of IN738 have been studied as a function of environment. Creep tests were conducted in air, both with and without a deposited layer of 25% NaCl/75% $Na_2SO_4$. In the presence of this deposited layer the steady state creep rate in air at $850^{\circ}C$ and 275 to 375 MPa increased by about 100%, while increases ranging from 90 to 170% were found at 307 MPa and 750 to $950^{\circ}C$. The effect of the deposited layer and the stress and temperature dependence of the steady state creep rate was little, although its presence led to marked decreases in the rupture lives.

The fatigue life determined in terms of cyclic plastic strain markedly decreased as the environment became more severe, in sequence from vacuum to air to $NaCl+Na_2SO_4$ deposited layer. The large strain rate effect found in the air and hot corrosion environments disappeared when the experiments were conducted in a vacuum of $1.3 \times 10^{-2}$ Pa.

## Introduction

Hot corrosion in gas turbines limits the durability of even the best blade materials at present available. It is caused by molten sulphate and chloride deposits. The hot corrosion of superalloys for turbine blade and vane applications in a simulated turbine environment has been studied for many years now. However, this kind of study is generally performed at elevated temperature with no stress. The influence of hot corrosion on the deformation and fracture of superalloys has been rarely studied (1), in spite of the potential importance of interaction between hot corrosion and mechanical properties.

This present work has been undertaken to clarify the relation between the hot corrosion and the creep, low-cycle fatigue behaviour of cast nickel-base superalloy. To this end, the creep and low-cycle fatigue properties of IN738LC were studied in some environments simulating conditions of industrial relevance.

## Experimental Procedure

The experiments were carried out on the nickel-base alloy IN738LC supplied by Messrs. Wiggin in the form of 76 mm dia. cast sticks which were then recast by Howmet Co. in the form of oversized specimens and lastly machined to size. Table 1 gives their chemical composition. The heat treatment schedules consisted of 2 hours at 1120°C in vacuum or hydrogen followed

Table I. Chemical Composition of the Alloy

| Co | Cr | Al | Ta | W | Mo | Ti | Nb | Zr | B | C | Ni |
|------|------|------|------|------|------|------|------|------|-------|------|---------|
| 8.30 | 15.9 | 3.40 | 1.72 | 2.50 | 1.60 | 3.30 | 0.96 | 0.07 | 0.012 | 0.12 | balance |

by cooling to room temperature, then 24 hours at 845°C in argon or vacuum followed by cooling to room temperature.

Some specimens were coated with the mixture of 25% NaCl+75% $Na_2SO_4$ by preheating to 150°C and then rotating the specimen in a saltwater spray until an even coating of 9.5 mg/cm$^2$ was obtained.

The alloy was tested using Denison Mod. T48 creep machines at temperature of 750 to 950°C and stresses of 196-375 MPa. The temperature was measured with two thermocouples placed at each end. The stability of the furnace temperature during creep tests was about ±1°C. An inductive transducer could detect strain variations as small as $2 \cdot 10^{-6}$ monitored by an automatically operated printer.

L.C.F. tests were carried out by a 25T closed-loop servohydraulic MTS system, in which a stainless steel vacuum chamber containing the specimen assembly was installed. A vacuum of the order of $1.3 \times 10^{-2}$ Pa could be achieved. The specimen was induction heated by a water-cooled copper coil fed by an R.F. generator. Temperatures were measured and controlled by thermocouples spot welded to each specimen near its minimum diameter. A diametral extensometer was placed on the specimen and all tests were carried out in diametral strain control at 900°C and at strain rate $10^{-2}$ or $10^{-3}$ s$^{-1}$ with
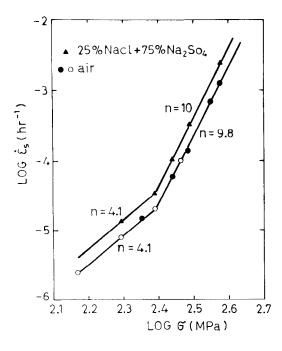
triangular wave form and with a mean strain of zero. During testing, the load and temperature were continually monitored and hysteresis loops were recorded at appropriate intervals.

The standard metallographic method was used to examine the microstructure of surface layer and to measure the thickness of the surface oxide. Electron probe microanalysis was used to measure concentration of elements in cracks and grain boundaries. After low-cycle fatigue testing, specimens were also extensively examined by scanning electron microscopy. The fractured specimens were sectioned on a plane containing the stress axis and crack initiation site, in order to examine microstructural features as well as the relationship between the crack path and the microstructure.

## Experimental Results

### Effect of Hot Corrosion on the Stress- and Temperature-Dependence of the Steady-State Creep Rate.

The relation between the steady-state creep rate and applied stresses at 850°C is given in Fig.1. The data in Fig.1 may be divided into two regimes, one at high stress levels and the other at low. The slopes of the curves are 9.8 and 4.1 respectively for air tests, and they are 10 and 4.1 for exposure in $25\%NaCl+75\%Na_2SO_4$ environment. It is clear that hot corrosion environment studied increases steady-state rate by about 100%, but does not change the stress-dependence, compared with that obtained from tests in air.
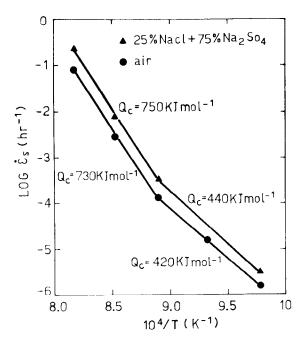


Figure 1 - The effect of hot corrosion on the stress dependence of the steady creep rate at 850°C. Open points from Ref.2.

Figure 2 - The effect of hot corrosion on the temperature dependence of the steady-state creep rate at 307 MPa.
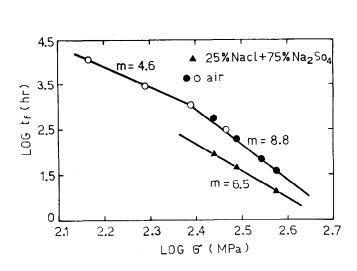
691

The temperature-dependence of steady-state creep rate at 307 MPa and 750-950°C is shown in Fig.2. At high stress levels a large activation energy is obtained (730 KJ mol$^{-1}$), while at low stress levels a smaller activation energy (420 KJ mol$^{-1}$) is found for air exposure. For hot corrosion exposure, values of activation energy correspond to 750 and 440 KJ mol$^{-1}$, respectively. The results show that there is very little difference between the two environmental exposures, although the steady-state creep rate in the hot corrosion environment increased by 90-170% over that in air (3).

## Effect of Hot Corrosion on the Stress- and Temperature-Dependence of the Time to Fracture.

As found for a wide range of metals and alloys, the time to fracture was then related to the steady creep rate as $t_f \propto K/\dot{\varepsilon}_s$. The stress- and temperature-dependence of the creep live of IN738LC can be described (6) as

$$t_f = A'\sigma^{-m}\exp(Q_f/RT) \qquad (1)$$

At 850°C the rupture lives are shorter in hot corrosion environment than in air by 65-85%, depending on applied stress. The lower the applied stress, the more severe the degradation. But the slope m of the curve in Fig.3 is slightly reduced, although it is still higher than the m value at low stresses.
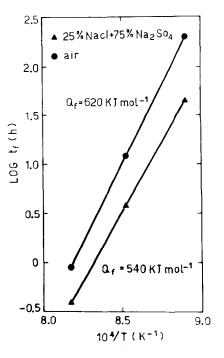




Figure 3 – The effect of hot corrosion on the stress dependence of the time to fracture for IN738LC at 850°C. Open symbols from Ref.2.

Figure 4 – The effect of hot corrosion on the temperature dependence of the time to fracture for IN738LC at 307MPa.

Similarly, the influence of the hot corrosion on activation energy $Q_f$ is very small (Fig.4). Actually the activation energies in the hot corrosion environment and in air are close to each other (within 10%), the former being slightly smaller than the latter (3).

## Effect of Hot Corrosion on L.C.F. Behaviour

The diametral strain range was converted to the longitudinal total strain range $\Delta\varepsilon_t$, the longitudinal plastic strain range $\Delta\varepsilon_p$ and the longitudinal elastic strain range $\Delta\varepsilon_e$. The data determined from an analysis of the hysteresis loop at approximately half the fatigue life are found to have a linear relationship between the three types of strain ranges and the cycles to crack initiation at a given strain rate, independent of the test environment, whether it is air, vacuum or a deposited layer of NaCl plus $Na_2SO_4$.

It can be seen from Fig.5 that air and NaCl+$Na_2SO_4$ deposited layer markedly decrease fatigue life determined in terms of cyclic plastic strain, compared with similar tests in vacuum, and this influence of saline environment on fatigue life is most severe.

Fig.5 shows that vacuum can eliminate the effect of strain rate, while in air or in hot corrosion environments there is a marked strain rate effect, i.e. when strain rate is decreased, the fatigue life is increased. Such an increase is not generally expected if one thinks in terms of a negative creep/fatigue interaction (4).
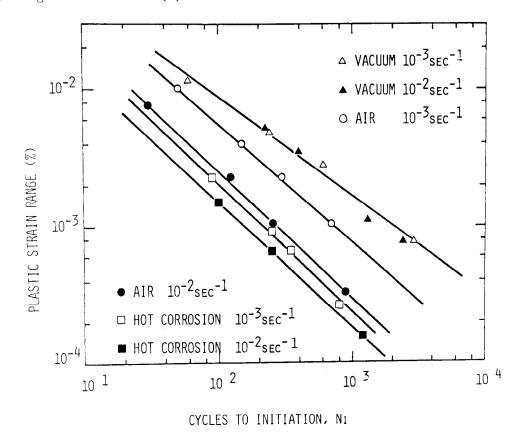


Figure 5 - The effect of environments on LCF behaviour of IN738LC at 900°C.
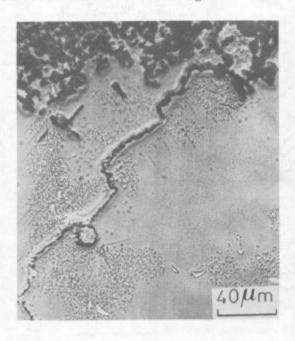
## Discussion

### Effect of Hot Corrosion on Creep Behaviour

The stator and rotor blades of gas turbine are prone to failure by hot corrosion, which is associated with $Na_2SO_4$ deposition on the blade surface. $Na_2SO_4$ has been shown to be less effective on creep properties of IN738LC than NaCl. However in the presence of NaCl rapid corrosion proceeds.

The metallographic observation showed that the surface oxide thickness is of the order of 60 μm, whereas the reduction in steady-state creep rate and rupture life would require a loss in section of some 130 and 310 μm (3) respectively. The effect must be obviously related to grain boundary corrosion. This is in agreement with results previously obtained by one of authors (Guo Jianting) for a 35Ni-15Cr iron-base superalloy (5). NaCl continually disrupts any protective oxide scales that form, allowing $Na_2SO_4$ to contact the underlying metal surface, and $Na_2SO_4$ promotes internal attack, particularly in regions adjacent to grain boundaries. It has been clearly seen in Fig.6b that the sulphidation proceeds along grain boundary into metal, which is shown by electron microprobe analysis. The combination of NaCl, $Na_2SO_4$ and applied stress makes the alloy suffer so severe hot corrosion.

In another work of ours (6), it has been pointed out that at high stresses for IN738LC, the dislocations generated at a source may bow between the γ' particles, and at low stresses, the dislocations created may be forced to surmount the γ' particles by climb. From above-mentioned results, it is concluded that the hot corrosion resulted essentially in no change in the creep mechanism. The deformation localized to grain boundary may slightly increase, because grain boundaries were made weaker by the hot corrosion. In addition, the loss in section through surface corrosion and grain boundary cracking



a. BSE                                      b. Distribution of S

Figure 6 - Intergranular cracks and its X-ray images of S. The specimen was crept at 850°C and 307MPa in 75%NaCl + 25%$Na_2SO_4$ environment with duration 5 hrs.

must result in some increased stress. These are the reasons why the steady-state creep rate in hot corrosion exposure is about twice as large as that in air exposure.

## Effect of Hot Corrosion on Low Cycle Fatigue Behaviour

Metallographic and scanning electron microscopic observation showed that nucleation of fatigue cracks occurred in selective and favorably oriented grain for tests in vacuum, and crack propagation appearred to be transgranular. There were no pronounced and visible oxide or corrosion products in the fracture surface (Fig.7). For tests in air, crack nucleation essentially occurred along oxidized boundaries and sometimes initiated along favorably oriented dendritic structure. On the other hand, for tests in hot corrosion environment, nucleation of fatigue cracks always occurred by surface ridging (Fig.8) at selective grain boundaries in the form of wedge-shaped oxide and sulphide intrusions (Fig.9) which are generally perpendicular to stress axis. In contrast with tests in vacuum there are some oxide and corrosion products (Fig.10) in the fracture surface of specimens tested in air and hot corrosion environments. After a relatively short period of intergranular crack propagation the cracks of specimens tested in air and hot corrosion environments frequently became transgranular.

From the above mentioned results, it can be seen that because of the action of oxidation and corrosion, fatigue crack nucleation in vacuum occurred less easily than in air, while nucleation in air was less likely to occur than in presence of salt deposited layer.

The fatigue process is largely one of crack propagation. Under cyclic plastic deformation, protective films are unlikely to reform at an exposed crack tip because of the mechanical action of stress and the chemical action of NaCl on the scales in hot corrosion environment. Therefore hot corrosion
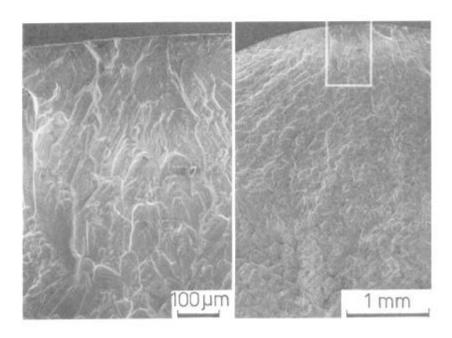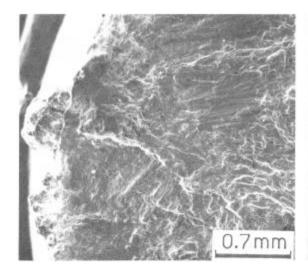


Figure 7 – Scanning electron micrograph of a fracture showing fatigue crack nucleation and propagation in vacuum (Ni=2900 cycles, $\Delta\varepsilon_p$=0.078%, $\dot{\varepsilon}$=10$^{-3}$ s$^{-1}$).
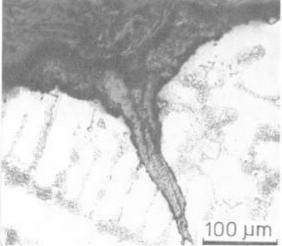
Figure 8 – Scanning electron micrograph of a fracture showing nucleation of fatigue crack by surface ridging ($N_i$=1200 cycles, $\Delta\varepsilon_p$=0.016%, $\dot{\varepsilon}$=10$^{-2}$s$^{-1}$).

Figure 9 – Intergranular nucleation and transgranular propagation of fatigue crack of specimen tested in hot corrosion environment ($N_i$=90 cycles, $\Delta\varepsilon_p$=0.23%, $\dot{\varepsilon}$=10$^{-3}$s$^{-1}$).
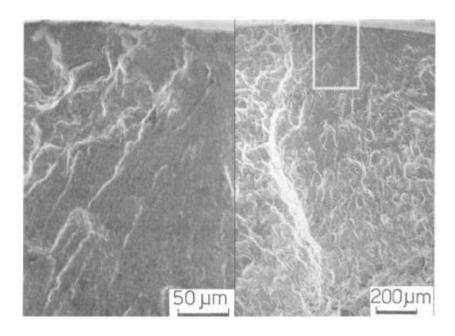


Figure 10 – Scanning electron micrograph showing oxide in fracture surface in air ($N_i$ = 700 cycles, $\Delta\varepsilon_p$ = 0.104%, $\dot{\varepsilon}$ = 10$^{-3}$s$^{-1}$).

proceeds continuously, and propagation of fatigue cracks is uninterrupted and transgranular. In air, however, crack propagation shows distinct differences. Although in this case brittle protective oxide films ($Cr_2O_3$) are ruptured under cyclic deformation, oxidation proceeds slowly and then protective films are reformed. With fatigue, this process of straining, film rupture and oxidation occurs repeatedly. It is quite evident that the effect of oxidation in air on fatigue crack propagation is less severe than that of hot corrosion environment. Thus hot corrosion environment resulted in a marked decrease in fatigue lifetimes represented on the basis of plastic strain (Fig.5), compared with similar tests in air.

Since vacuum eliminates environmental effects, there is no embrittled zone at a crack tip; each increment of crack advance will be substantially smaller for the unaffected plastic zone of the vacuum experiments, than for the embrittled oxidized or hot-corroded crack tip developed in the presence of air or 25% NaCl + 75% $Na_2SO_4$ deposited layer. This accounts for the substantial difference in fatigue life determined in terms of cyclic plastic deformation between tests in vacuum and air or hot corrosion environments.

## Conclusions

1. Hot corrosion severely reduced rupture lives and increased steady-state creep rate of the cast superalloy IN738LC.

2. The hot corrosion (induced from 25%NaCl/75%$Na_2SO_4$) did not change the stress- and temperature-dependence of the steady-state creep rate, so it resulted essentially in no change in the creep mechanism. The weakening of the grain boundary may slightly increase the likelihood of grain boundary sliding.

3. The high-temperature LCF properties ($\Delta\varepsilon_t$, $\Delta\varepsilon_e$ and $\Delta\varepsilon_p$) of IN738LC can be represented by the Coffin-Manson equation at a given strain rate, regardless of vacuum, air or deposited layer of NaCl/$Na_2SO_4$.

4. A comparison of the experimental results of experiments conducted in air, hot corrosion environment and vacuum on IN738LC at 900°C at two different strain rates shows not only a substantial increase in fatigue life, but also the disappearance of the effect of strain rate in a vacuum of $1.3 \times 10^{-2}$Pa.

5. Hot corrosion saline environment resulted in a marked decrease in LCF properties, compared with similar tests in air, and this decrease was greater at lower values of strain rate.

6. For tests in vacuum crack nucleation always occurred in favorably oriented grain, and for similar tests in air, crack nucleation essentially occurred along oxidized grain boundaries, but sometimes cracks were also initiated along selective dendritic structure, while for tests in hot corrosion environment, cracks always initiated by surface ridging at selective grain boundaries. All three undergo transgranular propagation.

## Reference

(1) J.R.Nicholls, J.Samuel, R.C.Hurst and P.Hancock, "The Influence of Hot Corrosion and Oxidation on the High Temperature Creep Behaviour of 316 Stainless Steel and Nimonic 108," pp.911-926 in Behaviour of High

Temperature Alloys in Aggressive Environments, I.Kirman et al. ed.; TMS, London, 1980.

(2) F.Schubert, A.V.D.Steinen and H.Brandis, COST-50, D-2/1, Final Report, Febr. 1977, Thyssen Edelstahlwerke AG, Krefeld, BRD.

(3) Guo Jianting, D.Ranucci, E.Picco, and P.M.Strocchi, "The Effect of Hot Corrosion on Creep and Fracture Behaviour of Cast Nickel-Based Superalloy IN738LC", pp.805-819 in High Temperature Alloys for Gas Turbines, R.Brunetaud, et al. ed.; D.Reidel Publishing Company, Dordrecht, 1982.

(4) Guo Jianting, D.Ranucci, E.Picco, and P.M.Strocchi, "Effect of Environment on Low-Cycle Fatigue Behaviour of Cast Nickel-Base Superalloy IN738LC," to be published.

(5) Guo Jianting, "An Investigation of the Oxidation and Hot Corrosion of a 35Ni-15Cr Type Iron-Base Alloy" Acta Metall. Sin. 15(2) (1979) pp.203-214.

(6) Guo Jianting, D.Ranucci, E.Picco, and P.M.Strocchi, "An Investigation on the Creep and Fracture Behaviour of Cast Nickel-Based Superalloy IN738LC," Met. Trans. A, being published in the near future.